# Resonant and nonresonant conduction-electron-spin transmission in normal metals

András Jánossy
*Laboratoire de Physique des Solides,* Université Paris-Sud, 91405 - Orsay, France*
*and Solid State Physics Department, Central Research Institute for Physics,*
*Post Office Box 49, H-1525 Budapest, Hungary*
(Received 16 May 1977; revised manuscript received 2 October 1979)

The propagation of nonequilibrium conduction-electron magnetization of paramagnetic metals under resonant and nonresonant conditions is described by a simple model and investigated experimentally. The theory is in qualitative agreement with the 9-GHz transmission experiments on high-purity paramagnetic metals coated with ferromagnetic layers to selectively enhance spin transmission. Observations on (i) the temperature dependence of the transmission electron-spin resonance (TESR) in Cu, Ag, and Au; (ii) on the anisotropy of the TESR at helium temperature in Cu, and Au; and (iii) a nonresonant single-particle spin-wave mode in Cu, Au, and W are reported. The nonresonant spin waves are attributed to ballistic electrons which cross the sample without momentum scattering. At low temperatures these waves give the major part of the nonequilibrium magnetization. Both transverse and longitudinal modes are observed.

## I. INTRODUCTION

By contrast with the early theoretical understanding of the elementary principles of the dynamics of isolated electronic spins in an insulator or a semiconductor, the basic description of the different phenomena involved in the magnetic resonance of conduction electrons in metals has been much slower in shaping up. As we want to establish here the nature of new observations of conduction-electron-spin excitation and propagation in normal, high-purity metals at low temperatures, a brief survey of the present situation is helpful.

The basic work of Dyson[1] provides a starting point for dealing with conduction-electron-spin dynamics in a metal. Dyson showed how the knowledge of the electron-gas correlation function entirely determines the response of the metal to an electromagnetic field. Although Dyson's method is general, it was applied in early works only to the case, valid in presence of strong momentum scattering, where a diffusion equation is used to represent the propagation of magnetization in the metal. Since then new developments have taken place along two main directions: (i) by inclusion of Fermi-liquid effects, i.e., electron-electron interactions, (ii) by taking into account nonresonant spin modes, appearing in the weak-scattering limit, when "ballistic" rather than "diffusive" propagation of electrons occurs.

Fermi-liquid effects were first demonstrated experimentally on sodium and potassium with the occurrence of paramagnetic spin waves.[2] The full theoretical description of these effects[3,4] pointed to the existence of many more higher-order modes for possible observation. So far only alkali metals have been investigated for these effects[2,5] and very recently aluminum.[6] In this type of work the anisotropy of the interactions between electrons is taken care of but a spherical Fermi surface was generally assumed except for the work of Walker.[7]

The prediction of the phenomenon of spin-resonance transmission was made by Azbel *et al.*[8] with a formalism equivalent to that of Dyson. Although the same authors[9] pointed out the importance of the orbital motion of the electrons, leading in particular to anisotropic diffusion, it was not realized until recently[10] that spin excitations of a single group of electrons and their subsequent coherent propagation can yield observable changes of the magnetization. Teitelbaum[11] has made a detailed investigation of this phenomenon which takes place at low temperatures in very pure metals when the collision mean free path becomes larger than the cyclotron orbit diameter. The corresponding phenomena for the propagation of electromagnetic currents along the orbit of the carriers has been described by Gantmakher and Kaner[12,13] for arbitrary Fermi surfaces. Furthermore Teitelbaum included isotropic Fermi-liquid effects in the propagation parameters thus covering a large number of situations, however specific application to the transmission geometry is lacking.

Experimentally, as noted by Teitelbaum[11] and Wilson and Fredkin[4] many of these spin signals are likely to be obscured if not washed out by the occurrence of much more intense excitation of orbital waves.[14] In this respect very promising progress has been achieved experimentally by the systematic use of the ferromagnetic sandwich geometry.[15] This technique enables one to enhance considerably the strength of the spin excitations of a metal leaving the orbital currents unchanged. Although the microscopic description of the ferromagnetic-paramagnetic boun-

dary is lacking, a consistent phenomenological model exists[16] allowing a simple interpretation of the modification of the paramagnetic resonance when excited by the ferromagnetic resonance of a film (rather than by direct electromagnetic radiation). With this technique we were able to investigate[10] the spin excitations of a single group of electrons otherwise unobservable on the "bare" metal in identical geometry.

In order to explain consistently our observations we derive here a simple theoretical model applying to free electrons on a spherical Fermi surface in the case of weak scattering. We show that in addition to the anisotropy of the ESR predicted by Azbel *et al.*[9] a nonresonant propagation appears which is the spin analogue of cyclotron waves. The model contains several simplifications and does not take into account the effect of a $g$-factor anisotropy and — more important — the effect of Fermi-liquid interactions.

The effect of Fermi-liquid interactions, Fermi-surface anisotropy, and $g$-factor anisotropy on the nonresonant spin modes has been investigated in detail in a recent work by Montgomery and Walker.[17] We have left out of this brief discussion some more specialized effects due to the finite size of the sample investigated: in the diffusion regime collisions on the surface with spin flip give rise to surface relaxation[1]; other purely geometrical effects arise[18] in the case where electrons can propagate over distances comparable to or larger than all dimensions of the sample. Nevertheless, it is in agreement with most of the experimental findings presented in Sec. III where we report on spin transmission observed under various conditions. The method of enhancing the spin transmission by coating paramagnetic metal foils with thin ferromagnetic layers allows us to investigate, besides the ESR around the resonance field, the ESR at fields far from the resonance, the anisotropy of the ESR in relatively thick foils, and nonresonant modes related to the energy spectrum of the electrons. Most of the investigations are on copper but some observations on silver, gold, and tungsten are also reported.

## II. PROPAGATION OF CONDUCTION-ELECTRON MAGNETIZATION IN A METAL

The main question dealt with in this paper is the following: What is the distribution of the spin magnetization induced by a radio-frequency field in a metal in a strong static magnetic field?

We shall not attempt to construct a theory taking into account all details of the excitation of magnetic modes and all complications of the orbital motion. Instead, we shall limit ourselves to a simple treatment by appropriately modifying Dyson's theory.[1] Our principal aim is to point out the qualitative differences in the spin propagation for different ranges of exciting frequencies, Larmor frequencies, and spin and momentum relaxation rates.

### A. Dyson's theory

Consider a metal occupying the $z>0$ half space in a static magnetic field $H_0$ oriented in an arbitrary direction (Fig. 1). A radio-frequency field $\vec{h}e^{-i\omega t}+$c.c. is incident on the metal surface. This field is strongly inhomogeneous, it is shielded within a short distance from the surface. The electrons are rapidly moving in the metal and when they come into the skin region they sense a rapidly varying field. In all the following we use the term polarization when describing the motion of a single-electron moment in contrast to the term magnetization which is the macroscopic quantity. Following Dyson[1] we first calculate the polarization of a single electron and then sum up for the different trajectories. The polarization of a single electron is assumed to obey a simple Bloch equation

$$\frac{d\vec{m}}{dt}=\vec{m}\times\vec{H}(t)-\frac{\vec{m}-\vec{m}_0}{T_1}\ , \tag{1}$$

where $T_1$ is a phenomenological relaxation time, $\vec{H}(t)=\vec{H}_0+\vec{h}(r(t))e^{-i\omega t}+$ c.c. is the sum of the static magnetic field and radio-frequency field effectively felt by the electrons moving in the metal, $m_0=\chi H_0$ is the equilbrium magnetization. Neglecting second-order terms in the nonequilibrium magnetization and introducing circular variables

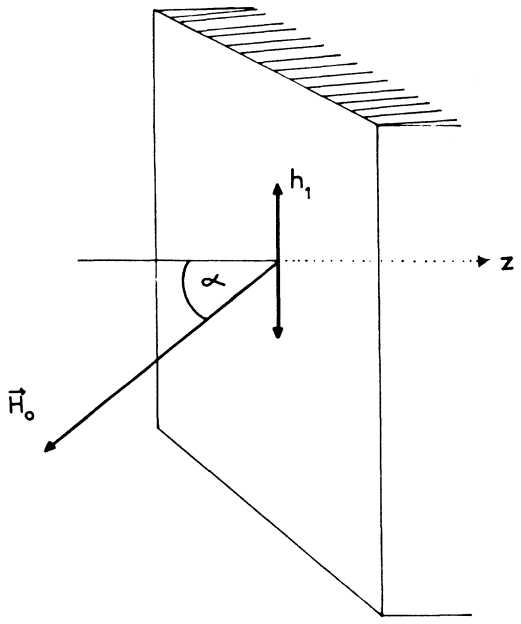


FIG. 1. Geometry of exciting ($h_1$) and static magnetic fields ($H_0$). $H_0$ is inclined by the angle $\alpha$ to the sample normal. $h_1$ is polarized in a plane perpendicular to $H_0$.

$m = m_{x'} + im_{y'}$, $h = h_{x'} + ih_{y'}$ (the $x'y'$ plane being normal to $H_0$) the solution of the differential equation (1) is

$$m_\omega = e^{-i\omega t}\chi\left(i\omega_0 + \frac{1}{T_1}\right)\int_{-\infty}^{t} h(\vec{r}(t'))\exp\left[-\left(i(\omega_0-\omega)+\frac{1}{T_1}\right)(t-t')\right]dt' ,$$

$$m_{-\omega} = e^{i\omega t}\chi\left(i\omega_0 + \frac{1}{T_1}\right)\int_{-\infty}^{t} h^*(\vec{r}(t'))\exp\left[-\left(i(\omega_0+\omega)+\frac{1}{T_1}\right)(t-t')\right]dt' , \quad (2)$$

$$m = m_\omega + m_{-\omega} ,$$

where $\omega_0 = \gamma H_0$ is the Larmor frequency. In the following we shall keep only the term $m_\omega$ and abandon the subscript $\omega$ for brevity. We note, however, that far from resonance both terms are equally important. We average over different electron trajectories $\vec{r}(t)$ by introducing the correlation function $G(t,t',\vec{r},\vec{r}')\,d\vec{r}'$, the probability that an electron which is at time $t$ in $\vec{r}$, was at a previous time $t'$ in the volume $d\vec{r}'$ around $\vec{r}'$.

In pure metals and in the frequency range of interest the skin depth is very short. The average time an electron spends in the skin region is orders of magnitude shorter than the period of the Larmor precession $2\pi/\omega_0$ or the period of excitation $2\pi/\omega$. We assume that all electrons passing the skin region are excited in the same way independently of their momentum. This is certainly a crude approximation but it greatly simplifies the problem and allows us to neglect details of the excitation. We assume for simplicity that the exciting field always decays exponentially with a wave vector $(C\delta)^{-1}$ where $C$ is a complex number of order of unity. If $\delta$ is sufficiently small the magnetization of the whole system is

$$m(\vec{r},t) = A\int_{-\infty}^{t} G(t,t',\vec{r},0) \times \exp\left[-\left(i(\omega_0-\omega)+\frac{1}{T_1}\right)(t-t')\right]dt' , \quad (3)$$

$$A = e^{-i\omega t}\chi\left(i\omega_0+\frac{1}{T_1}\right)C\delta h .$$

When $\omega \neq \omega_0$ the integrand is rapidly oscillating and averages to zero if the correlation function is varying smoothly. This is the case for electrons described as diffusing free particles where the magnetization is large only at the ESR, $\omega = \omega_0$. However, when the mean free path of electrons becomes long the correlation function may not be taken as smoothly varying and any peaks in it lead to waves in the magnetization.

### B. Electron-spin resonance

The motion of electrons was described by Dyson[1] as a diffusion of free particles all having the same velocity magnitude $v_F$. In doing this the effect of the static field on the motion was neglected and $\omega_c\tau \ll 1$ was assumed ($\omega_c$ is the cyclotron frequency and $\tau$ the momentum relaxation rate). This restriction was removed by Azbel *et al.*[9] and was also treated by Lampe and Platzman.[19] As these authors showed in the case of $\omega_c\tau \gg 1$ the motion may still be described by a diffusion but with an anisotropic diffusion constant: the effective momentum mean free path along the magnetic field is unchanged ($\lambda_\parallel = v_F\tau$) but in the plane perpendicular to the magnetic field it is strongly reduced and in the limit of a very long momentum relaxation rate it is of the order of an average electron orbit radius ($\lambda_\perp \approx r_c = v_F/\omega_c$). In this model the diffusion of electrons in the plane perpendicular to the magnetic field is replaced by the diffusion of the center of orbits.

Taking for the correlation function $G$ the solution of the one-dimensional diffusion equation, Eq. (3) may then be integrated[20]

$$m = A\frac{T_1}{\delta_{\text{eff}}}\frac{\exp\{-(z\sqrt{2}/\delta_{\text{eff}})[1+i(\omega-\omega_0)T_1]^{1/2}\}}{[1+i(\omega-\omega_0)T_1]^{1/2}} , \quad (4a)$$

$$\delta_{\text{eff}} = (2DT_1)^{1/2} , \quad (4b)$$

$$D = \tfrac{1}{3}v_F^2\tau\left(\cos^2\alpha + \frac{\sin^2\alpha}{1+\omega_c^2\tau^2}\right) , \quad (4c)$$

where $\alpha$ is the angle of the magnetic field to the surface normal.

A simple picture was given by Lewis and Carver[20] to understand the above expression. Electrons arriving at the skin region become slightly polarized perpendicularly to both the static and rf fields. The electrons cross rapidly the skin and maintain their polarization for a relatively long time $T_1$. This polarization precesses in the external static field $H_0$ with a phase determined by the phase of the rf field at the time of excitation. As electrons are diffusing the polarization of electrons at a given point is destroyed by strong interference in general. However, at the ESR all spins precess in phase and the magnetization propagates into the metal as a uniform mode. The distance of penetration, the spin mean free path $\delta_{\text{eff}} = (2DT_1)^{1/2}$ is determined by both the momentum and spin-relaxation times. Off resonance, $(\omega-\omega_0)\,T_1 \gg 1$, the magnetization is attenuated by

the phase spread of the polarization and not by spin relaxation. The magnetization is no more uniform but oscillates with a wave vector independent of $T_1$

$$k_{\text{off resonance}} = \left(\frac{\omega_0-\omega}{D}\right)^{1/2}(1-i) \quad . \tag{5}$$

Off resonance the tail of the ESR is very strongly decreasing with frequency since its square root appears in the exponential.

### C. Nonresonant transverse magnetization (Larmor waves)

In the above analysis it was implicitly assumed that variations of the magnetization over the momentum mean free path may be neglected. This is not the case if $|\omega-\omega_0|\tau \gg 1$ and we shall show that under this condition the diffusion model does not hold.

Consider the spatial distribution of the transverse magnetization of electrons all having the same momentum vector (i.e., those corresponding to a given point on the Fermi surface) but excited at different times. We neglect for the moment relaxation and take the static magnetic field perpendicular to the surface. These electrons give rise to a Larmor wave[10] with a wave vector

$$k = \frac{\omega_0-\omega}{v_H} \quad , \tag{6}$$

where $v_H$ is the velocity component along the magnetic field. This is easily understood by considering the extreme cases $\omega \ll \omega_0$, $\omega \gg \omega_0$, and the ESR $\omega = \omega_0$.

If $\omega \ll \omega_0$ the phase of the excitation is slowly varying and all electrons may be considered as excited with the same phase. As electrons leave the skin their polarization precesses with the Larmor frequency and since all are moving with the same velocity component along the static magnetic field, they give rise to a wave with $k \cong +\omega_0/v_H$.

If $\omega \gg \omega_0$ the precession of the polarization inside the metal may be neglected but the electrons become excited with different phases in different times and the wave vector is $k \cong -\omega/v_H$. (The minus sign comes from the choice of the sense of rotation of the exciting field.)

At $\omega = \omega_0$ there is no difference between a Larmor wave and the ESR, the change of phase of the Larmor precession is counterbalanced by the rotation of phase of the excitation and the wave vector is zero.

The total magnetization of the system is obtained by summing over the Fermi surface. To take into account momentum scattering we group electrons into two parts: the "ballistic" electrons, which arrive from the skin region at the distance $z$ without momentum scattering and the "diffusing" electrons which have lost momentum memory. This distinction may not be always clear, especially for complicated Fermi surfaces where the use of a single momentum relaxation rate may not be justified.

Electrons scattered at least once give rise to the ESR and we describe them within the diffusion model while the ballistic electrons give rise to Larmor waves. According to this we modify Eq. (3)

$$m(\vec{r},t) = A\int_{-\infty}^{t}[G_d(t,t',\vec{r},0)e^{-(t-t')/T_1} + G_b(t,t',\vec{r},0)e^{-(t-t')/\tau}]e^{-i(\omega_0-\omega)(t-t')}dt' \quad , \tag{7}$$

where $G_d$ stands for the correlation function of diffusing and $G_b$ of the ballistic electrons. We add to Eq. (7) the normalizing condition

$$\int_V [G_d(t,t',\vec{r},0)\,(1-e^{-(t-t')/\tau}) + G_b(t,t',\vec{r},0)]\,d\vec{r} = 1 \quad . \tag{8}$$

In the term describing ballistic electrons in Eq. (7) the spin relaxation is not included explicitly. We note that for spin-orbit relaxation (the dominant relaxation mechanism in pure metals) every spin-flip process is accompanied by a momentum scattering[21] and so the factor $\exp[-(t-t')/\tau]$ takes into account spin relaxation.

### D. Nonresonant transverse magnetization for a spherical Fermi surface

For a spherical Fermi surface $G_b$ has a very simple form

$$G_b(t,t',z,0) = \frac{1}{v_F(t-t')}, \quad \text{if } z < v_F(t-t') \quad ,$$
$$G_b = 0, \quad \text{if } z > v_F(t-t') \quad . \tag{9}$$

The step in $G_b$ at $t-t' = z/v_F$ results in an oscillating magnetization which has a particularly simple form for large distances from the surface, $z \gg \lambda = v_F\tau$, and the static magnetic field perpendicular to the surface

$$m \approx A\frac{\tau \exp\{-z[1/\tau + i(\omega-\omega_0)]/v_F\}}{z[1+i(\omega_0-\omega)\tau]} \quad . \tag{10}$$

The wavelength of the oscillations are determined by $v_F$, the maximum velocity component along the magnetic field. For Fermi surfaces not too much distorted from spherical $G_b$ is still expected to have a jump at the minimum transit time $t-t' = z/v_F$ and

the magnetization oscillations are determined by the Fermi velocity of tip electrons towards which the magnetic field is pointing.

One of the most important features of Eq. (10) is that although the magnetization is a sum of waves with different wavelengths, the phase spread of electrons with different velocity components $v_H$ results only in a linear attenuation with the difference in exciting and Larmor frequencies. Since the ESR decays exponentially with the square root of frequency the magnetization of Larmor waves is larger than the tail of the ESR for sufficiently long momentum relaxation times. From Eqs. (4a) and (10) the condition for the Larmor wave oscillation amplitude to be larger than the tail of the ESR is approximately

$$3|\omega_0-\omega|\tau>1 \ . \tag{11}$$

For magnetic fields tilted from the surface normal the cyclotron motion can not be neglected. However, electrons with a velocity component $v_H$ close to $v_F$ have the smallest orbit radii for a Fermi surface not strongly different from spherical and so give rise to the least phase smearing. For not too strongly tilted fields Eq. (10) is expected to remain valid if $z$ is replaced by $z/\cos\alpha$.

In the above considerations we limited ourselves to calculating the magnetization for large distances from the exciting surface, e.g., $z>v_F\tau$. For small distances two important complications arise: (a) for frequencies close to the ESR the normalizing condition Eq. (8) can not be neglected; (b) the approximation in obtaining Eq. (10) from the general expression (7) is not valid anymore. We have not investigated in detail the consequences of these approximations for $z<v_F\tau$ since our principal aim was to give a simple model to explain qualitatively the experiments.

### E. Longitudinal waves

In Secs. II A–II D we described waves where the nonequilibrium magnetization is perpendicular to the direction of propagation, i.e., these are transverse modes. There may exist longitudinal modes also[4] where the nonequilibrium magnetization points along the propagation. This polarization is not precessing with the Larmor frequency so, from the argument of Sec. III C, its wavelength $2\pi v_H/\omega$ is independent of the static field magnitude. However, since small exciting fields give rise to a polarization perpendicular to the exciting and static magnetic field such modes can be excited only under special conditions discussed in Sec. IV G.

### F. Transmission through slabs of finite thickness

In the transmission experiments, described in the following, the measured quantity is the rf magnetic field transmitted through a metal slab of thickness $l$. The sample is placed between two cavities which act as polarizers. The exciting field is linearly polarized and only the component of the field at the second surface polarized in the direction of the exciting field polarization is detected. The transmitted rf field is proportional to the corresponding component of the magnetization at the emitting surface.[20]

To calculate the magnetization for finite sample thicknesses the spin and momentum scattering at the boundaries must be specified. We may assume that surface spin relaxation is small while momentum is diffusely scattered. In this model the magnetization of Larmor waves is unaffected by the finiteness of the sample, on the other hand the ESR increases for thicknesses less than $\delta_{\text{eff}}$ since it becomes a sum of reflected waves.

### G. Concluding remarks

We may classify the different possibilities for conduction-electron-spin penetration in a metal according to Table I. We have not taken into consideration the effects of a $g$-factor anisotropy on the magnetization distribution. The $g$-factor anisotropy has only a limited effect on the ESR (both for isotropic and anisotropic diffusion) since the ESR is the result of the coherence of the precession of electrons over the spin-relaxation time $T_1$. $T_1$ is usually much larger than $\tau$ and the effect of the $g$-factor anisotropy in broadening the resonance is reduced by motional narrowing.

Larmor waves depend on the details of the Fermi surface, the oscillations vary with crystal and magnetic field orientation. Metals with very large $g$-factor anisotropies, so that no ESR is hoped for, may still exhibit magnetization oscillations characteristic of the nonresonant spin transmission of a particular group of electrons on the Fermi surface.

The Larmor waves, just as cyclotron waves, are of a great variety. The transverse spin modes discussed in Sec. III C propagate along the magnetic field and are analogous to the Ganthmaker-Kaner oscilla-

TABLE I. Classification of conduction-electron-spin penetration modes in a pure metal.

| $\omega_c\tau$ | $\lvert\omega-\omega_0\rvert T_1$ | $\lvert\omega-\omega_0\rvert\tau$ | Dominant mode |
|---|---|---|---|
| $\ll 1$ | $\lesssim 1$ | $\ll 1$ | ESR (isotropic $D$) |
| $>1$ | $\lesssim 1$ | $\ll 1$ | ESR (anisotropic $D$) |
| $\gtrsim 1$ | $>1$ | $<1$ | "tail" of ESR (decaying with frequency) |
| $>1$ | $>1$ | $>1$ | Larmor waves |

tions.[13] Spin modes propagating perpendicular to the magnetic field related to the Ganthmaker size effect also exist although these are more complicated as they depend on the phase coherence of both currents and magnetization.

*Longitudinal* spin waves, i.e., waves polarized parallel to the static field, exist for low frequencies in contrast to longitudinal current modes which are excited only above the plasma frequency since they are accompanied with a non-neutral charge density distribution.

## III. OBSERVATION OF CONDUCTION-ELECTRON-SPIN TRANSMISSION IN FERROMAGNETIC-PARAMAGNETIC METAL SANDWICHES

### A. Apparatus

The experiments were performed on a standard *X*-band (9 GHz) transmission-electron-spin-resonance (TESR) spectrometer,[22] Fig. 2. The microwaves after amplitude modulation at 100 kHz are fed into the emit cavity. The metal sample constitutes a common wall of the emit and receive cavities and is much thicker than the skin depth. If there are weakly attenuated modes carried by the conduction electrons then a small part of the field is transmitted into the receive cavity. The cavities are rectangular, operated in the $TE_{101}$ mode and are filled with $Al_2O_3$ blocks ($\epsilon \approx 10$) to reduce size. The exciting and transmitted rf magnetic fields are at the surfaces of the sample and are parallel to each other. The static field may be rotated in a plane perpendicular to the rf magnetic field from parallel to perpendicular to the sample surface (Fig. 1). Field strength may be varied form 0 to 7 kG. The transmitted rf field is mixed with a reference field taken from the same oscillator as the main power and then detected. By means of a variable phase shifter in the reference arm the phase of the detected signal may be chosen at will. The phase may also be continuously rotated by a motor, in this case the contour of the signal is proportional to the amplitude of the field transmitted into the receive cavity (power spectrum).

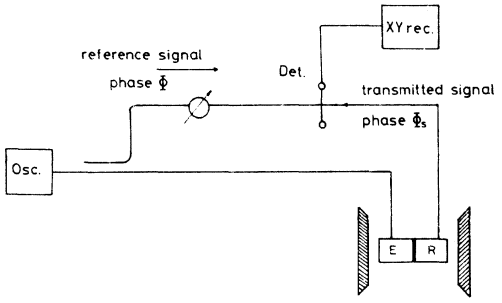


FIG. 2. Principle of TESR spectrometer. Osc.: 9.2-GHz oscillator; Φ reference phase; Det: mixer and detector; E: emit cavity; R: receive cavity.

### B. Sample preparation

The transmission properties of high-purity copper, silver, gold, and tungsten were investigated. We describe in detail observations on copper and discuss to a much lesser extent the results on the other metals.

The characteristics of the copper samples are given in Table II. The high-purity copper and gold single crystals were grown in an induction furnace and then cut with a spark machine. The copper single-crystal slices were annealed in low pressure ($10^{-4}$ Torr) air, the gold in air at atmospheric pressure, at temperatures near the melting point (~1000 °C). The polycrystalline copper, silver, and gold foils[23] were of somewhat lower purity. The resistivity ratio between room temperature and 4 K for samples before annealing was 1000 to 2000. This was greatly increased by the air anneal as seen by the large increase of microwave transmission at low temperatures. The perfection of the samples was somewhat deteriorated by clamping them between the cavities. The high-purity tungsten single crystal was supplied by Dr. B. Maxfield, Cornell Univ., Ithaca, New York.

The samples were coated usually on both faces with a thin layer of an amorphous ferromagnetic alloy of cobalt and phosphorus (Co-P). One 50-$\mu$m copper sample was plated on only one face. The samples were tried for transmission coated and uncoated and in some cases samples were recoated and run for a third time. The Co-P layers were electrolytically deposited onto the chemically etched metals in a bath described in Ref. 24. The thickness of the Co-P layers was typically 0.4 $\mu$m, much less than the skin depth of Co-P which is about 5 $\mu$m.

The ferromagnetic resonance (FMR) of the Co-P layers deposited onto the samples was measured by standard reflection techniques. The FMR is relatively broad, the linewidth for magnetic field parallel to

TABLE II. Characteristics of copper samples.

| Name | Thickness ($\mu$m) | Orientation[b] normal to surface | Plane of rotation of $H_0$ |
|---|---|---|---|
| Cu 1, 2, 3[a] | 50 | Polycrystalline | ··· |
| Cu 4 | 260 | [110] | (001), (110) |
| Cu 5 | 295 | [100] | (001) |
| Cu 6 | 697 | [100] | (001) |

[a]Cu 1,2,3 are three different samples made of the same foil.
[b]Orientation of the crystals was within 5° of the stated values.

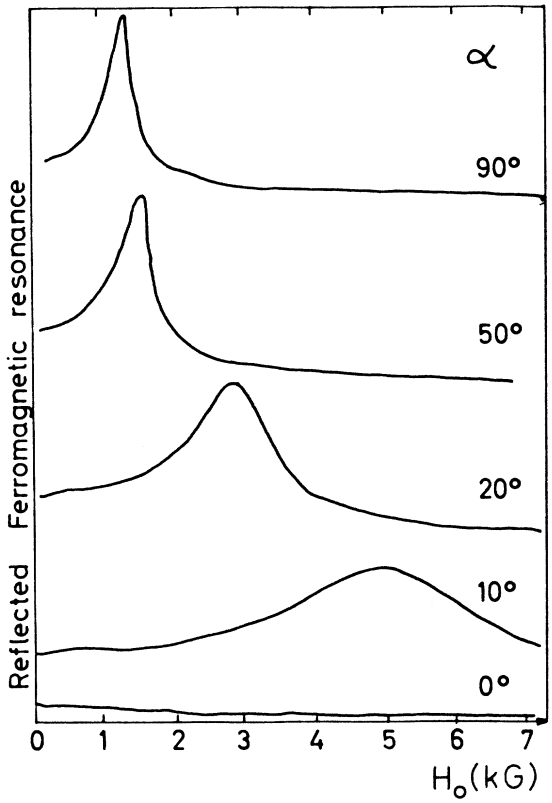


FIG. 3. Variation of the (reflected) ferromagnetic resonance of a typical amorphous Co-P layer with static magnetic field angle. $\alpha = 90°$ corresponds to $H_0$ parallel, $\alpha = 0°$ to $H_0$ perpendicular to the sample. For $\alpha = 0°$ the demagnetizing fields shift the FMR to about 12 kG and so it is not observed in the present experiments.

the sample is typically 400 G. The Curie temperature of the layers was much higher than room temperature and no significant change in the FMR was observed down to helium temperature. The saturation magnetization is high ($4\pi M$ is around 10 kG[24]) and the demagnetization fields strongly shift the FMR. Experimental traces of the FMR versus the angle of the static magnetic field to the surface normal is shown on Fig. 3.

The FMR width, and to a less extent resonance field depend on details of the sample preparation and are not perfectly reproducible. Co-P layers deposited onto very smooth surfaces showed resonances as narrow as 75 G.

In Secs. III C–III I we report observations on copper and in Sec. III J on the silver, gold, and tungsten samples.

### C. Transmission in uncoated copper

Our results on the TESR of uncoated copper agrees with those reported in the literature.[25] For thin samples (50 $\mu$m) the line shape is Lorentzian at low temperatures. Above 20 K the spectrum is independent of magnetic field orientation. Lubzens *et al.*[26] reported anisotropies with crystal and magnetic field orientations at low temperatures. However, the presence of a strong cyclotron wave transmission[25] makes observations difficult to analyze. The low-temperature residual linewidth for our samples was independent of thickness and was between 15 and 25 G depending on the perfection of the crystals. At higher temperatures the linewidth rapidly increases and deviations from the Lorentzian shape occur: minima appear on both sides of the central maximum. The 295-$\mu$m-thick sample showed a non-Lorentzian line shape even at 20 K with a maximum to minimum ($A/B$) ratio of 2.5. The ESR was not detected on the uncoated 697-$\mu$m-thick sample.

At low temperatures a large variety of transmission signals appears in the whole magnetic field range swept and the spectrum is usually very complicated. In some crystal and magnetic field orientations the spectrum is oscillatory. One of the best known type of such oscillations is the high-frequency Ganthmaker-Kaner oscillation.[13,14]

### D. TESR at high temperatures of Co-P-coated copper

The observation of an enhanced TESR in copper foils one face coated with a soft ferromagnetic permalloy layer was reported.[15] The present observations on the 50-$\mu$m-thick copper plated on one face with Co-P are very similar to that found with permalloy, the enhancements and additional linewidths are about the same. To obtain a larger enhancement of the spin transmission we coated all other samples on both sides. The main features of the transmission spectra of these samples at temperatures above 20 K are the following.

The transmission at the TESR has a $g$ factor equal to that of uncoated copper. The enhancement of the intensity (measured by the linewidth times the amplitude) of the plated sample TESR compared to the unplated one is several hundreds for magnetic fields parallel or perpendicular to the sample and a few thousands when the FMR occurs at the same magnetic field as the TESR. This enhancement is of the order of the square of that of one surface coated samples. The phase of the enhanced TESR depends on the difference in frequencies of the ferromagnetic and conduction-electron resonances.[16] The phase of TESR changes with the magnetic field orientation by somewhat less than $2\pi$ for both sides coated samples. The linewidth is increased and this increase is about twice that observed for one surface coated samples. The broadening is inversely proportional to sample thickness and gives usually the main contribution to the linewidth. It is about 100 G per plated surface for a 100-$\mu$m thickness.

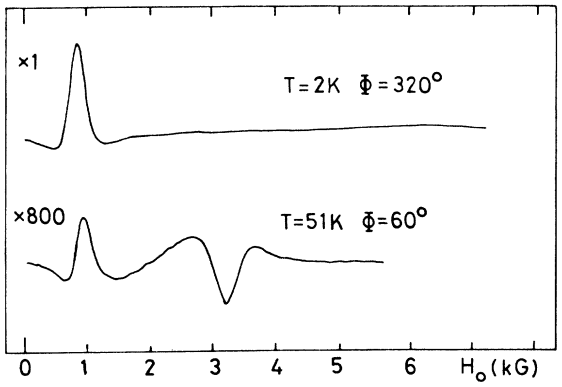


FIG. 4. Transmitted ferromagnetic resonance (TFMR). The sample is a 50-$\mu$m-thick polycrystalline copper foil plated on both surfaces with thin Co-P layers. The static magnetic field is oriented parallel to the sample. At 2 K the TFMR is much more intense than the TESR (which is not visible with this amplification), at 51 K the TFMR (signal at 1 kG) has comparable intensity to the TESR at 3.2 kG. Note the difference of the reference phase $\Phi$ at the two temperatures.

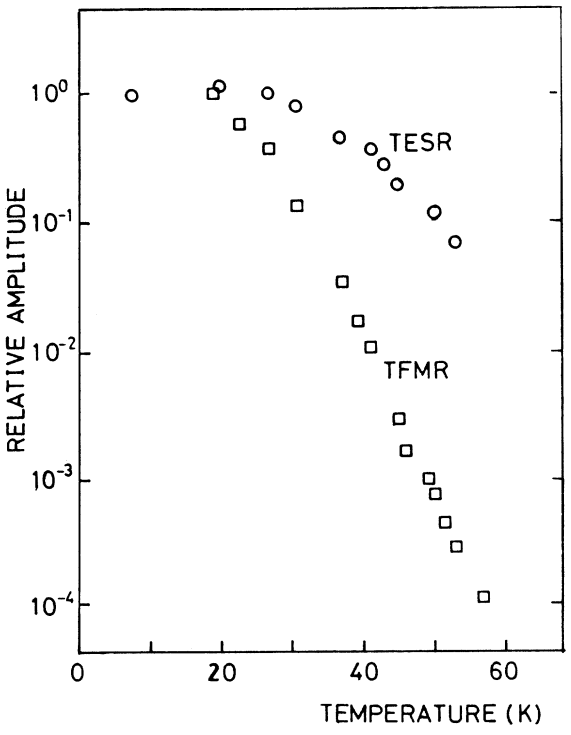


FIG. 5. Variation of the amplitude of the TESR and the TFMR vs temperature. The amplitudes are normalized to 1 at 1.5 K. Same sample and same magnetic field orientation as for Fig. 4.

### E. Transmitted FMR

While thick foils of copper (270 $\mu$m or thicker) show at high temperatures only the TESR described above, the spectrum of the 50-$\mu$m thick sample consists of two peaks. In addition to the TESR a strong transmission peak occurs at the FMR field (Fig. 4). We term this *transmitted ferromagnetic resonance* (TFMR) but noting, however, that we shall attribute it to a spin transmission by conduction electrons of the paramagnetic metal (see Sec. IV C).

The linewidth of the TFMR is about as large as the FMR of the Co-P layers. In spite of this, the enhanced transmission can not be explained by a modulation of the microwave leakage around the sample at the FMR of the Co-P layers which at low temperatures is typically three orders of magnitude weaker than the observed signals.

For the 50-$\mu$m-thick copper sample the TFMR signal is much more intense than the TESR at 2 K. The TFMR amplitude decreases much faster with temperature than the TESR (Fig. 5) and at 50 K they are of comparable amplitude (Fig. 4). Together with the amplitude the phase of the TFMR shifts also with temperature; the same TFMR line shape is observed at all temperatures if the reference phase is appropriately adjusted. This phase change is not of instrumental origin since it does not occur for the TESR.

### F. Low-temperature anisotropy of the TESR in Co-P-plated copper

At low temperatures (<15 K) the TESR is superimposed on an intense oscillating spectrum described in Sec. III G. However, the TESR amplitude is comparable or larger than that of the oscillations and so it may be clearly observed. This is in contrast to the nonenhanced case where the cyclotron background is typically an order of magnitude stronger than the TESR in pure metals.

The TESR of the 50-$\mu$m-thick sample is not changing below 20 K. On the other hand, the thick samples (260, 295, 697 $\mu$m) show a striking anisotropy effect: the TESR amplitude decreases sharply when the magnetic field is oriented within a few degrees from parallel to the surface (Fig. 6). For the 295-$\mu$m-thick copper sample the amplitude of the TESR at exactly parallel fields was 200 times smaller than 20 degrees off parallel (Fig. 7). The TESR of the 697-$\mu$m-thick sample could not be detected at parallel, however, at a few degrees off parallel it is visible. The ratio of the amplitude of the center of the line to the side minima ($A/B$ ratio) decreases as the field approaches parallel. The phase of the remaining signal at parallel is different from that at magnetic fields tilted a few degrees off parallel, phase changes up to

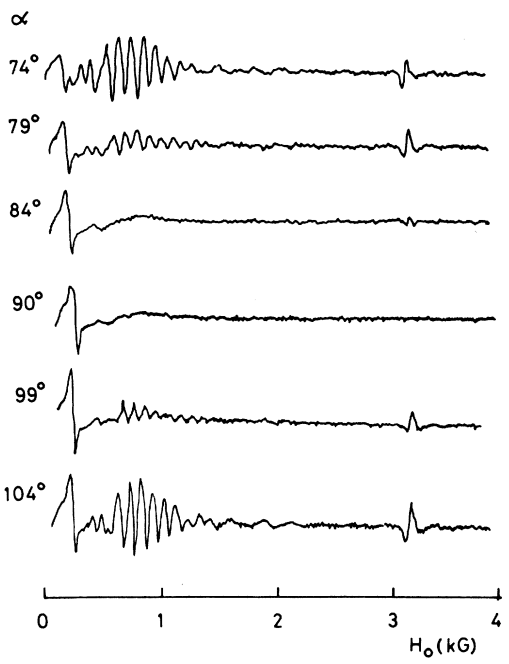


FIG. 6. Anisotropy of the TESR for field oriented near to parallel to the surface. Co-P-coated copper, thickness 697 $\mu$m. $\alpha = 90°$ corresponds to $H_0$ parallel to the sample surface and pointing in the [100] direction. The disappearance of the TESR (signal at 3.2 kG) for $\alpha = 90°$ is explained by the anisotropy of the spin diffusion. Note the phase change of the TESR indicating many-body effects. The low-field oscillations are transverse Larmor waves enhanced around the FMR of the coating layers. The signal at about 200 G visible in all spectra is attributed to Ganthmaker size effect and is not spin transmission.

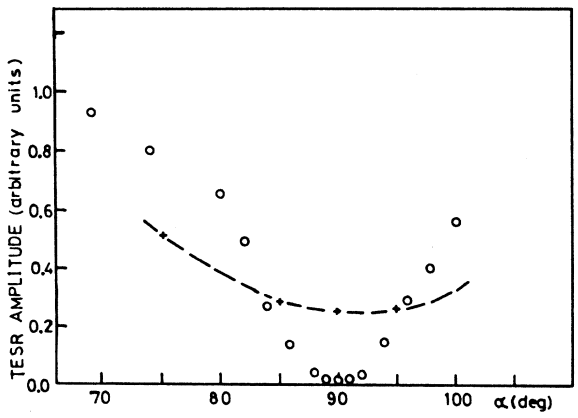


FIG. 7. Anisotropy of the TESR amplitude. $\alpha$ is the angle between static field and sample normal. (○): $T = 4$ K; (+): $T = 22$ K. The sample is a 295-$\mu$m-thick Cu single crystal both faces coated with Co-P. At $T = 4$ K the amplitude is strongly reduced when $\alpha = 90°$, i.e., $H_0$ parallel to sample surface.

about $\frac{1}{2}\pi$ were observed (Fig. 6).

When increasing the temperature the intensity of the TESR at parallel magnetic field increases while a few degrees off parallel it slightly decreases. The anisotropy disappears between 15 and 20 K (Fig. 7).

### G. Oscillating transmission of coated samples at low temperatures

The thick coated samples show below 15 K for nearly all magnetic field orientations a spectrum oscillating over the whole magnetic field range available. This type of spectrum is very different from the uncoated sample spectrum. Even in those cases where the uncoated sample spectra are periodic the periods of coated and uncoated sample spectra are different (Fig. 8). The amplitude of the oscillations increases around the FMR and TESR fields. This is best seen on the power spectrum where the transmitted field amplitude is measured. The phase of the oscillations varies around the FMR but not around the TESR. The oscillation period is well defined and depends on crystallographic and magnetic field orientation and is inversely proportional to sample thickness (Fig. 9).

It is important to discriminate whether the oscillations appearing in Figs. 8 and 9 are due to a change of amplitude of the transmitted field or whether they are due to a linear rotation of phase $\phi_s$ (see Fig. 2) of the transmitted signal with static magnetic field (of

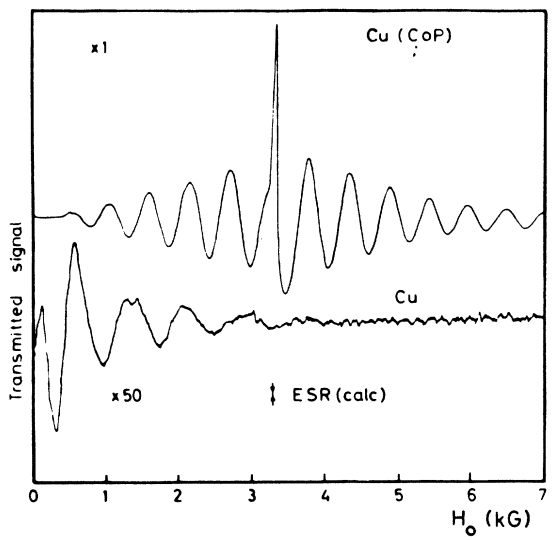


FIG. 8. Transmission spectra of a Cu single crystal. Upper trace: Enhanced spin transmission of sample both faces coated with Co-P layers. Lower trace: Ganthmaker-Kaner oscillations of the same crystal without coating. Sample thickness: 697 $\mu$m, magnetic field oriented normal to sample surface and parallel to the [100] direction. (Reproduced from Ref. 4.)

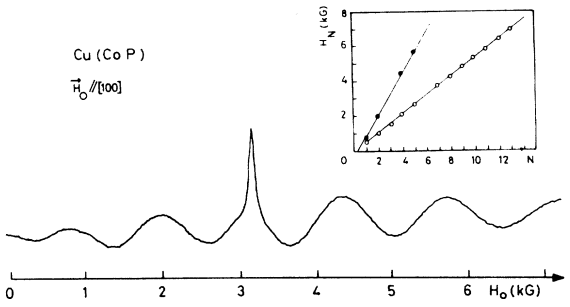


FIG. 9. Larmor waves in a copper single crystal. Both surfaces are coated with Co-P. The thickness is 295 $\mu$m and $H_0$ is perpendicular to the sample, in the [100] direction. Insert: position of the field $H_N$ for oscillation maximum as a function of maxima number $N$. Full circle: geometry of the present sample; open circle: geometry of the sample of Fig. 8.

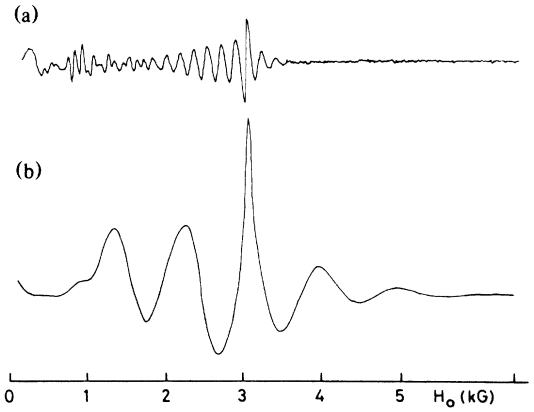


FIG. 11. Larmor waves oscillations at tilted magnetic field in CoP-plated copper single crystals. (a) sample thickness 697 $\mu$m, $\alpha = 45°$ $H_0$ // [110], the oscillations are well defined around the TESR at 3.2 kG. At low field the oscillations are more complicated. (b) thickness 260 $\mu$m, $\alpha = 45°$, $H_0$ // [100].

which only the projection on a reference rf field of phase $\phi$ is measured). In order to test this we changed the phase $\phi$ of the rf reference by $\Delta\phi$. The oscillations observed are identical in amplitude but shifted in magnetic field position. As the phase change of the observed oscillations at a given static field position is just the phase change $\Delta\phi$ of the rf reference we conclude that the origin of the oscillations is a linear rotation of the transmitted magnetization with the magnetic field strength.

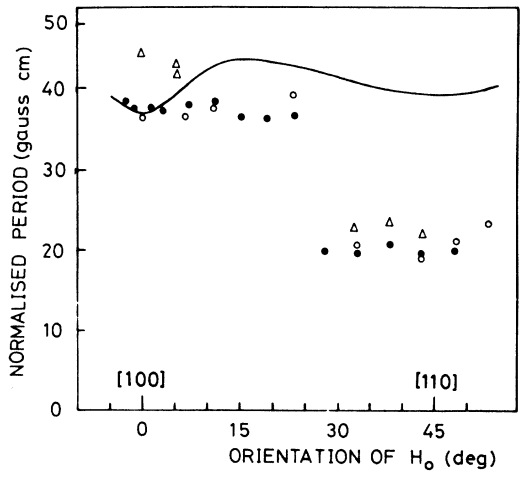


FIG. 10. Normalized Larmor oscillation period $\Delta H_{Lw} l/\cos\alpha$ vs magnetic field orientation with respect to crystal orientation. The magnetic field is rotated in the (100) plane. $l$: sample thickness; $\alpha$: magnetic field orientation with respect to sample normal. The continuous curve is calculated from the Halse data using the "tip" electron model. Δ: $l = 273$ $\mu$m; ●: $l = 295$ $\mu$m; ○: $l = 697$ $\mu$m; ●, ○: surface normal in the [100] direction. Δ: surface normal in the [110] direction. Cu single crystals, both surfaces coated with Co-P.

In the particular case of magnetic field oriented in the [100] direction perpendicular to the sample (Cu 5 and Cu 6 of Table II) the period of the oscillations is very well defined over the whole spectrum. In other geometries the situation is more complicated, often oscillations with different periods are superimposed. The oscillations are well defined for several periods around the TESR when the magnetic field is tilted less than $\alpha = 50°$–$60°$ from the sample normal. This period was measured for the magnetic field rotated in the (100) plane for two different crystal orientations and different thicknesses. The oscillation period multiplied by $l/\cos\alpha$ (where $l$ is the sample thickness) is shown on Fig. 10. Clearly the oscillation period is inversely proportional to the sample thickness and is shorther for magnetic fields more tilted towards parallel. Near parallel some oscillations with very short period are observed together with other long period oscillations (Fig. 11).

The amplitude of the oscillations is comparable with the amplitude of the ESR and in some geometries it is difficult to separate them.

While the period is independent of temperature the amplitude decreases strongly in the temperature region where the electronic mean free path becomes short (15–20 K). The decrease of the oscillation amplitude is much faster than the decrease of the ESR amplitude.

### H. Nonoscillatory low-temperature transmission

In addition to the above described oscillatory transmission a broad nonoscillating transmission is also observed at low temperatures. The nonoscillato-

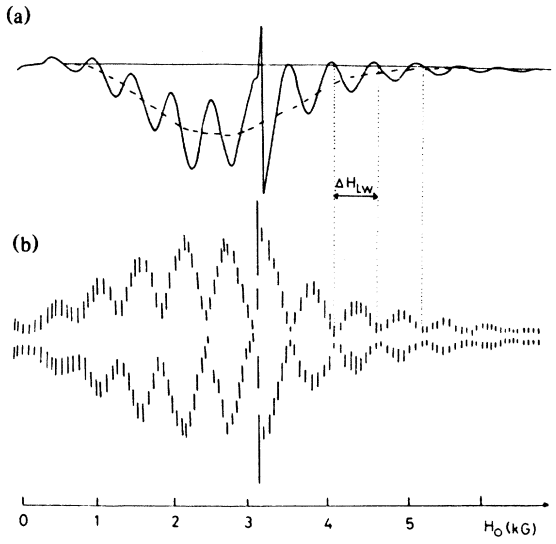


FIG. 12. Superposition of oscillating (transverse) and nonoscillating (longitudinal) Larmor waves. (a) Spectrum taken with fixed reference phase. The dashed curve indicates the nonoscillating component. (b) Power spectrum. The reference phase is continuously rotated. Only the contour of the spectrum is indicated. The full period of the fixed phase spectrum $\Delta H_{Lw}$ is equal to the magnetic field change between two minima in the power spectrum as indicated by the dotted lines.

ry transmission is peaked at the FMR field and is best identified for thick samples and field orientations of $\alpha = 5°$ to 40° from the sample normal. A typical spectrum showing the superimposed oscillatory and nonoscillatory transmissions of the 697-$\mu$m-thick sample is shown on Fig. 12. At magnetic fields perpendicular to the sample nonoscillatory transmission does not appear (within the range of 7 kG). The power spectrum is smoothly varying in this case. For $\alpha = 10°$, shown on Fig. 12, the nonoscillating transmission is well defined and the power spectrum is oscillatory with a distance between the minima equal to a full period of the oscillations of the spectrum taken with fixed reference phase.

The nonoscillatory transmission is distinguished from the TFMR in that the temperature dependence of its amplitude follows closely that of the oscillations and for a given static field no phase change is observed with the variation of temperature. The TFMR is strongest for parallel magnetic fields and for thin samples. The thick samples show very little transmission at parallel magnetic fields. Although the distinction between the nonoscillatory transmission and the TFMR may seem to be somewhat arbitrary, especially for thin foils, we think, however, that these reflect two very different mechanisms for spin propagation.

### I. Spin transmission in silver, gold, and tungsten

The transmission spectra of the 50-$\mu$m-thick polycrystalline silver foil both sides plated with Co-P layers are in every respect similar to those of copper of the same thickness. This is well represented by the similar variation of the TFMR phase versus amplitude at high temperatures.

The TESR of gold could not be identified without enhancement by ferromagnetic layers. The properties of the enhanced TESR[27] are similar to that in copper and silver. The temperature dependence of the intrinsic linewidth is very strong, it varies from 200 to 2000 G between 4 and 20 K. Both the TFMR and the TESR were observed in the 100-$\mu$m-thick sample at parallel static field, but only the TFMR is resolved in the 25-$\mu$m-thick one. The amplitude of the TFMR is decreasing strongly with temperature but no significant variation of its phase was observed although it was detected up to 30 K. The TESR is anisotropic around parallel fields in the thicker samples (100, 260, and 490 $\mu$m) at low temperatures. Both oscillatory and nonoscillatory enhanced transmission were observed in these samples.[27]

In the 400-$\mu$m-thick tungsten single crystal no TESR could be identified, on the other hand

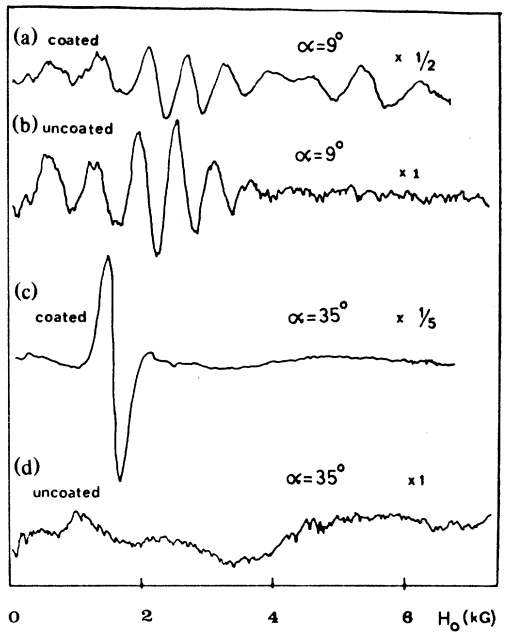


FIG. 13. Transmission spectra of tungsten. Thickness 400 $\mu$m, $\alpha$ is measured in the $(1\bar{1}0)$ plane from the [110] direction normal to the sample. The oscillations of (a) and (b) below 4 kG are similar and are due to cyclotron waves. In (a) above 4 kG, where spin enhancement is large, Larmor oscillations appear. At $\alpha = 35°$ (spectrum c), the strong transmission around the FMR may be due to longitudinal Larmor waves.

TABLE III. Summary of observed features in the transmission spectra of Co-P-plated metals.

| Sample thickness ($\mu$m) | High temperature Isotropic ESR | TFMR[a] | Low temperature Anisotropic ESR[c] | Nonresonant transmission[b] |
|---|---|---|---|---|
| Copper | | | | |
| 50 | + | + | − | − |
| 260 | + | − | + | + |
| 295 | + | − | + | + |
| 697 | + | − | + | + |
| Silver | | | | |
| 50 | + | + | − | − |
| Gold | | | | |
| 25 | − | + | − | − |
| 100 | + | + | + | + |
| 260 | + | − | + | + |
| 490 | + | − | + | + |
| Tungsten | | | | |
| 400 | − | − | − | + |

[a]At $H_0$ parallel to sample surface.
[b]Oscillatory and nonoscillatory.
[c]Near $H_0$ parallel to sample surface.

enhanced nonresonant transmission was found. The transmission of coated samples is enhanced around the FMR and the oscillations of coated and uncoated samples have different periodicities as appears in Fig. 13.

We summarize the different phenomena observed in the various metals in Table III.

## IV. DISCUSSION

The transmission spectra of the ferromagnetic-paramagnetic sandwiches gives rise to two important questions: What is the mechanism of the excitation? What are the excited modes?

### A. Enhancement of spin transmission

The answer to the first question is not clear. Stray radio-frequency fields around the ferromagnetic layers can not explain the enhanced signals since a very thin oxide layer between the ferromagnetic and paramagnetic layers prevents the coupling from being effective.[16] We believe that the coupling has a more microscopic origin and is a type of proximity effect between nonequilibrium magnetizations.[15,28] A detailed phenomenological theory based on this assumption has been presented by Silsbee, Jánossy, and Monod.[16]

According to this phenomenological theory the nonequilibrium magnetization of the layer excited by the microwave field incident on the sample gives rise to a magnetization at the surface of the following layer with a magnitude proportional to it. Experiments show[15,16] that in permalloy-copper sandwiches the coupling may be described as a transmission of some of the nonequilibrium magnetization between the ferromagnetic and paramagnetic layers. During the transmission through the interface the orientation of the transmitted magnetization does not change and the nonequilibrium magnetizations are parallel. The coupling in Co-P copper sandwiches shows the same characteristics as that of the permalloy-copper ones and we conclude that in this case the nonequilibrium magnetizations are also parallel at the interface.

The resulting transmission through a ferromagnetic-paramagnetic-ferromagnetic sandwich arises in this model in the following way: the incident microwave field induces a nonequilibrium ferromagnetic magnetization and — since the ferromagnetic layer is much thinner than its skin depth — excites the paramagnetic layer directly. However, the coupling between the ferromagnetic and paramagnetic magnetizations[15] gives rise to a paramagnetic magnetization one to two orders of magnitude larger than the direct excitation. The conduction electrons transmit the magnetization through the paramagnetic layer which is much thicker than its skin depth. At the second interface the ferromagnetic layer is excited by the coupling and emits an electromagnetic wave again one to two orders of magnitude stronger than the direct emission from the paramagnetic layer. As a result the enhancement of the transmission in samples both sides coated is the square of that in samples

one side coated with a ferromagnetic layer, and the normal excitation in the skin depth, although present, is negligible compared to the FMR coupled one.

In the following we adopt this simple picture, but noting, however, that it is only an approximation. The coupling not only enhances the spin transmission but gives rise to a spin cross relaxation of the conduction electrons of the paramagnetic metal.[15,16] This leads to a broadening of the TESR but has little effect on the nonresonant spin transmission which is not affected by surface relaxation if the momentum relaxation is diffuse at the surface.

### B. Nature of the excited modes

The rf transmission through uncoated metals is known to be due to the spin resonance and at low temperatures to cyclotron waves.[29] The nonresonant spin transmission is masked by the latter, the coupling in the skin of the rf field to currents is much stronger than to the conduction-electron magnetization. Moreover, the typical wavelengths, and hence the oscillation periods corresponding to the two modes, are comparable.

On the other hand we believe that most of the observed spectra of metals coated both sides with ferromagnetic layers arises from spin transmission. This is supported by the following observations:

(a) The spectra of coated samples are qualitatively different from uncoated ones. At low temperatures, even when oscillations appear in both cases, the periods are different.

(b) The intensity of the spectra of coated samples increases at the FMR, where the spin excitation is large, and around the TESR, where the penetration depth is large.

(c) The ferromagnetic layers do not change the excitation of the cyclotron waves significantly. In some cases where the spin enhancement is not particularly strong (far from the ESR and FMR) the cyclotron wave spectrum could be identified in both the plated and unplated samples with the same intensity and shape.

### C. Isotropic spin-diffusion regime ($\omega_c\tau \ll 1$)

In copper above 20 K the mean free path $v_F\tau$ becomes shorter than the maximum cyclotron orbit radius $v_F/\omega_c$ at 3 kG. In this temperature range both $\omega_c\tau < 1$ and $|\omega-\omega_0|\tau < 1$ are valid for the magnetic fields used in the experiments and the only mode of penetration of the conduction-electron magnetization is by isotropic spin diffusion.

According to this we attribute the two high-temperature transmission peaks observed in the 50-$\mu$m-thick copper and silver foils (Fig. 4) to the same mechanism: spin transmission in the diffusion regime. The TESR peak corresponds to the long penetration depth of the magnetization at the Larmor frequency, the TFMR corresponds to the tail of the ESR where the penetration depth is short but the excitation is very strong. The temperature dependence of the two peaks (Figs. 5 and 14) shows this clearly. As the temperature is increased the lattice vibrations shorten both the momentum and spin-relaxation rates. The penetration depth of the TESR at 20 K, $\delta_{\text{eff}} = v_F(\frac{2}{3}\tau T_1)^{1/2}$, is about 100 $\mu$m (depending somewhat on how the surface spin relaxation is taken into account), and that of the TFMR in the parallel-field geometry [$(\omega-\omega_0)/\gamma \approx 2$ kG], $\delta_{\text{TFMR}} = v_F[\frac{2}{3}\tau/(\omega-\omega_0)]^{1/2}$, is about 20 $\mu$m. The amplitude of the TESR does not change until $\delta_{\text{eff}} > l$ ($l$ is the sample thickness), the amplitude of the TFMR begins to decrease at much lower temperatures (Fig. 5) since $\delta_{\text{TFMR}} < l$ already at 20 K. The wave vector of the TESR at $\omega = \omega_0$ is real at all temperatures and so the phase of the transmitted field does not change with temperature. The wave vector of the TFMR [expression (5)] has equal real and imaginary parts and, as expected, not only the amplitude but also the phase of the TFMR changes with temperature. According to Eq. (5) the Néperian logarithm of the relative TFMR amplitude should be equal to the change of phase in rad. As appears in Fig. 14 this is the case for copper and silver at high temperatures (above 40 K for copper). At lower temperatures the TFMR amplitude increases faster

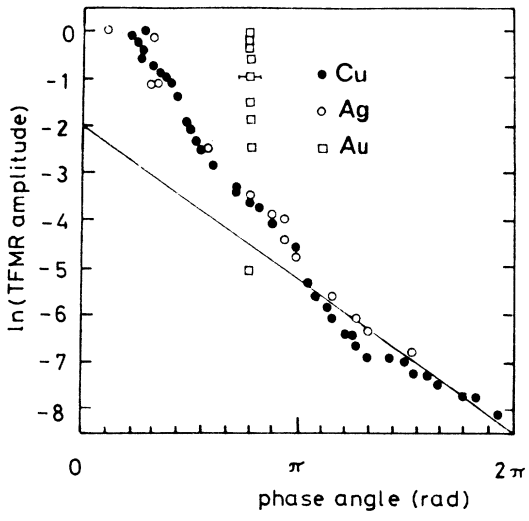


FIG. 14. Transmitted ferromagnetic resonance amplitude vs phase of transmitted field at maximum transmission. Cu and Ag thickness, 50 $\mu$m; Au thickness, 25 $\mu$m. Amplitudes normalized to 1 at 1.5 K. The static magnetic field is parallel to the sample. The straight line corresponds to the diffusion model.

than expected from the phase change. This deviation, as discussed in Sec. IV F, is probably explained by the breakdown of the diffusion model when $\omega_c\tau \ll 1$ and $|\omega-\omega_0|\tau \ll 1$ do not hold any more.

### D. TESR in the anisotropic diffusion regime [$\omega_c\tau > 1$, $|\omega-\omega_0| T_1 \ll 1$]

In pure metals at low temperatures and magnetic fields of a few kG the condition $\omega_c\tau \gg 1$ is fulfilled and the diffusion of electrons becomes anisotropic. This effect was taken into account by Schultz *et al.*[2] in the evaluation of the spin-wave spectra of alkali metals, but we know of no direct experimental verification on TESR. We explain the strong variation of the amplitude of the TESR with magnetic field angle, for fields nearly parallel to the surface (Sec. III F, Fig. 7) as a manifestation of the anisotropy of the spin diffusion. This anisotropy leads, for $H_0$ parallel to the surface, to a strong decrease of the spin penetration depth with temperature and to a geometrical effect due to the finite dimensions of the sample exposed to the microwave field. We attempt to analyze our data on the 295-$\mu$m-thick (Co-P-coated) copper sample by taking plausible values for the momentum relaxation rate. We consider only the free-electron model and neglect Fermi-liquid effects.[3,4]

We assume the following data:

$$\omega_c = 5.0 \times 10^{10}\ \text{sec}^{-1}\ ,$$

$$v_F = 1.0 \times 1.0^{8}\ \text{cm/sec}\ ,$$

$$\tau = 3 \times 10^{-11}\ \text{sec at 22 K}\ ;$$

$$\tau = 3 \times 10^{-10}\ \text{sec at 4 K}\ ,$$

and

$$T_1 = 7.5 \times 10^{-9}\ \text{sec}$$

independently of temperature below 22 K. The effect of broadening of the line due to coupling at the ferromagnetic-paramagnetic interface is important for $l/\delta_{\text{eff}} < 1$, while it may be omitted in a qualitative analysis if $l/\delta_{\text{eff}} > 1$.

With the above values the temperature and angular variation of the TESR amplitude for $H_0$ oriented close to parallel to the surface may be explained. For $H_0$ parallel to the surface the line shape is non-Lorentzian at all temperatures thus $l/\delta_{\text{eff}} > 1$ and interface broadening may be neglected. In this case from expressions (4b) and (4c) the effective spin-diffusion length is

$$\delta_{\text{eff}} = (\tfrac{2}{3} v_F^2 \tau T_1)^{1/2}/(1+\omega_c^2\tau^2)^{1/2}\ .$$

and inserting the above values: $l/\delta_{\text{eff}} = 1.4$ at $T = 22$ K and $l/\delta_{\text{eff}} = 3.8$ at $T = 4$ K. This explains part of the strong reduction of the amplitude of the TESR as the temperature is decreased.

The observed angular variation of the amplitude is also in qualitative agreement with the model. At 22 K $\omega_c\tau = 1.5$ and only little angular variation is expected. The observed smooth variation (Fig. 7) may be partly due to a change in the enhancement[15] also. At 4 K a sharp decrease is expected for angles near to $\alpha = 90°$ since $\omega_c\tau \approx 15$ and the diffusion coefficient varies rapidly with angle [expressions (4b) and (4c)]. On the other hand at $\alpha = 0°$ the spin transmission is along the magnetic field and $l/\delta_{\text{eff}} = 0.25$, thus a Lorentzian line shape is observed.

A further complication of the analysis arises from a geometrical effect noted by Pinkel and Schultz[18] in the TESR of high-purity alkali metals. At low temperatures and parallel magnetic field the electrons reaching the emitting surface diffuse along the static field to distances comparable to the cavity $d = 4$ mm in that direction. At 4 K the magnetization spreads beyond the edges of the cavity to about $\omega_c\tau\ l = 4.5$ mm and reduces the intensity of the observed TESR by a factor of about 3. This shielding effect depends strongly on the angle of magnetic field in the geometry considered above and it becomes negligible for $\alpha < 85°$ for the 295-$\mu$m sample (Fig. 15) as the geometrical "cutoff" angle determined by the ratio of the thickness to the width of the sample is close to 4.5°.

The observation of a strong anisotropy in qualitative agreement with the free-electron model, in the TESR in copper (and gold) shows that Fermi-liquid effects can not be very important in these metals. Exchange interaction alone leads to an isotropic diffusion of magnetization and thus tends to smooth the anisotropy.

We note that the observed change of the line shape and in particular the change of its phase with temperature at parallel magnetic fields can not be explained by the anisotropic spin-diffusion model.

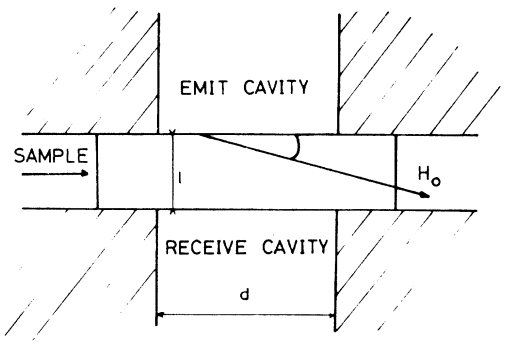


FIG. 15. Geometrical "window" effect reducing the TESR for $H_0$ parallel to sample surface. For $\omega_c\tau \gg 1$ the spin diffusion is anisotropic, electrons excited at the emit cavity surface diffuse preferentially along $H_0$ and before reaching the emit cavity surface flow out of the window determined by the cavities. The effect is important if $H_0$ is tilted less than $l/d$ from the surface.

Since the spatial variation of the magnetization is strongest in this geometry this is an indication of many-body effects.[6,30] An analysis of the variation of the phase shift with temperature and magnetic field orientation shows that the first Landau exchange coefficient $B_0$ is negative and $0.01 < |B_0| < 0.05$.

### E. Transverse Larmor waves

We attribute the low-temperature oscillations of the transmission spectra of coated samples (Sec. III G) to transverse Larmor waves described in Sec. II D. As discussed in that section the period of the oscillations $\Delta H_{\mathrm{Lw}}$ is determined by the velocity component along the magnetic field, $v_H^{\max}$ and the $g$ factor of electrons at a sharp change in the velocity distribution

$$\Delta H_{\mathrm{Lw}} = \frac{2\pi\hbar}{g\mu_{\mathrm{B}}} \frac{v_H^{\max}}{l} \cos\alpha \quad . \tag{12}$$

In principle $v_H^{\max}$ can be evaluated from the variation of the zero magnetic field phase $\phi_s$ of the oscillations with the sample thickness. This phase is determined by the time of flight of electrons across the sample and is independent of the $g$ factor. This method was applied by Baraff and Phillips[31] for the analog case of cyclotron waves. However the experimental indeterminacy in $\phi_s$ is large and the present data would not allow a determination of $v_H^{\max}$ from $\phi_s$ with an accuracy better than 10%. On the other hand $\Delta H_{\mathrm{Lw}}$ was measured with an accuracy of a few percent and in some orientations even better. Since the $g$-factor anisotropy of copper, obtained from an analysis of the frequency dependence of the linewidth of the TESR by Lubzens *et al.*,[26] is only a few percent, we take the $g$ factor to be equal to the mean value, i.e., that determined by the ESR, $g_{\mathrm{Cu}} = 2.033$.[25] We compare on Fig. 10 the measured values of $\Delta H_{\mathrm{Lw}} l / \cos\alpha$ to $2\pi\hbar v_F / g_{\mathrm{Cu}}\mu_{\mathrm{B}}$ calculated from the Fermi velocity data of Halse.[32] In cases where the oscillation period was not unique in the whole magnetic field range (Fig. 11) we take the period of oscillations around the ESR which is usually well defined. Most likely some oscillations in tilted magnetic fields are related to interferences due to the cyclotron motion neglected in our simple model. The cyclotron motion has the least effect on Larmor waves around the ESR where the Larmor wavelength is relatively long compared to the cyclotron orbit radius.

The theoretical period, as discussed in Ref. 10, is in a very good agreement with the measured one in the [100] direction. The agreement is somewhat less good but still satisfactory for orientations up to 25° tilted from the [100] direction towards the [110] direction (Fig. 10). In this range the experimental period is nearly constant, the calculated one varies about 10% and it seems that the Larmor wavelength is determined by "tip" electrons with a velocity component along the magnetic field close to $v_F$. Around the [110] direction the measured oscillation period is about half the calculated one showing that in this direction the simple model, based on an undistorted spherical Fermi surface, fails.

The temperature dependence of the spectrum agrees with the predictions of the model. At the lowest temperatures $\omega\tau$ is most probably between 10 and 20 and as the condition $|\omega - \omega_0|\tau > 1$ is fulfilled in nearly the whole magnetic field range, the harmonic oscillations dominate the spectrum. As the temperature is increased the TESR is little changed but the Larmor waves disappear rapidly since the penetration depth is equal to the momentum mean free path, which decreases more rapidly than the spin mean free path.

Some important discrepancies between experiment and theory remain to be explained. One of the most disturbing facts is that the observed Larmor waves appear to be always circularly polarized. The smooth variation of the power spectrum for perpendicularly oriented magnetic fields and the shift of the oscillations when the reference phase is changed, observed for all orientations, shows this clearly. The theory predicts a mainly circularly polarized wave only around the peak of the ESR and a linearly or at least ellipticaly polarized one otherwise, this discrepancy was observed for cyclotron waves in copper also.[14]

According to (Eq. 10) of Sec. II D the phase of the oscillations is expected to be inverted when passing through the TESR. Although Eq. (10) was obtained from a model of spherical Fermi surface, on physical grounds this is expected to remain approximately valid whenever Larmor waves are the result of an interference of waves with largely differing wavelengths. However, such an inversion of the phase was not found at any crystallographic or magnetic field orientation. We have no good explanation for these discrepancies. We note, however, that Eq. (10) is derived taking all electrons of the Fermi surface into account. If only a smaller group of electrons is retained, $G_b$ (Eq. 9) is modified towards single-particle behavior where phase inversion [appearing in the denominator of Eq. (10)] does not occur.

### F. Spin transmission related to the orbital size effect

At low temperatures the TFMR observed in the parallel field geometry in the 50-$\mu$m-thick copper sample is particularly strong (Fig. 4). The ratio of the TFMR amplitude to the TESR amplitude is larger by more than an order of magnitude than calculated from the diffusion model (Fig. 14). [The TESR is not decreased by the anisotropy of the diffusion since the diameter of the maximum cyclotron orbits (at $H_0 = 3$ kG) is of the order of the sample thickness.]

The most probable explanation of the strong TFMR is a spin transmission related to electrons with orbit diameters larger than the sample thickness and which cross the sample without scattering. The spread of time of flight and therefore of the spin polarization of nonscattered electrons is less than that of diffusing ones for samples much thinner than a typical orbit diameter. This explains the large amplitude of the TFMR and the small variation of its phase at low temperatures. The maximum orbit diameter at 800 G, a typical FMR field in the parallel geometry is 150 $\mu$m which is indeed much larger than the sample thickness, 50 $\mu$m. In agreement with this model no strong transmission is observed in the parallel geometry for thick ($\geq 270$ $\mu$m) samples.

It may be that the lack of any phase change with temperature of the TFMR of gold is explained by a spin transmission related to the orbital size effect at low temperatures while at higher temperatures by the ESR being so broad that $|\omega-\omega_0| T_1 < 1$ even at the FMR field (Fig. 14).

### G. Longitudinal waves

We suggest that the nonoscillating part of the low-temperature spectrum described in Sec. III H may be a transmission of longitudinal waves. Such waves were discussed by Wilson and Fredkin[4] theoretically. As noted in Sec. II E under the usual experimental conditions, where the spin system is directly excited by an external rf field, no longitudinal waves arise. However, it follows from experiments described in Ref. 16 that when the metal is excited via a ferromagnetic layer the excited paramagnetic magnetization is parallel to the ferromagnetic nonequilibrium magnetization. The rf ferromagnetic magnetization near to the FMR is ellipticaly polarized in the plane perpendicular to the equilibrium magnetization $M_f^0$. Since the directions of $M_f^0$ and $H_0$ are not coincident in general, the rf ferromagnetic magnetization and so the rf paramagnetic magnetization $M_p$ coupled to it, has a component parallel to the static field $H_0$ (Fig. 16) $M_p^{\parallel}$. In this interpretation the variation of the amplitude and phase of the nonoscillatory transmission reflects the variation of the component of the rf ferromagnetic magnetization parallel to the static field. There is no longitudinal excitation when $H_0$ is parallel to the sample because then $H_0$ and $M_f^0$ are parallel, on the other hand, it is expected to be strongest near perpendicular $H_0$ where the angle between $H_0$ and $M_f^0$ is the largest. This is confirmed by the experiments at magnetic field angles near perpendicular as long as the FMR occurs within the limited range of available field. Further tests are needed to confirm the nature of these excitations but it is our feeling that the present experimental evidences make our conclusions very likely.

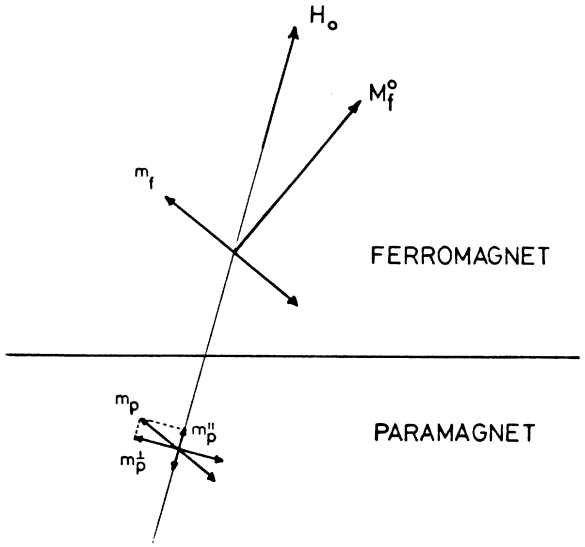


FIG. 16. Excitation of longitudinal waves in a ferromagnetic-paramagnetic metal sandwich. Due to demagnetizing fields the equilibrium ferromagnetic magnetization $M_f^0$ is not parallel to the external static magnetic field $H_0$. The excited ferromagnetic magnetization $m_f$ is perpendicular to the equilibrium magnetization. The excited paramagnetic magnetization $m_p$ is parallel to $m_f$ and has components longitudinal ($m_p^{\parallel}$) and transverse ($m_p^{\perp}$) to the static magnetic field $H_0$.

### H. Spin transmission in tungsten

The Larmor waves observed in tungsten are an example to show that in sufficiently pure metals, where the momentum mean free path is long, nonresonant spin transmission always occurs. On the other hand the failure to identify the ESR may be a consequence of a strong $g$-factor anisotropy. This is to be expected in a heavy metal with a relatively complicated band structure like tungsten. A detailed analysis of the nonoscillatory spin transmission of tungsten in terms of longitudinal Larmor waves has been presented recently by Jánossy and Kollár.[33]

## V. CONCLUSIONS

We have developed a model to show that in paramagnetic metals an anomalous penetration of conduction-electron magnetization occurs under the same conditions as for the anomalous penetration of currents. The model is in agreement with the main findings of our experiments on paramagnetic metals coated by ferromagnetic layers on both surfaces. In these sandwich samples the spin transmission is greatly enhanced and the dynamics of the conduction-electron magnetization could be investi-

gated not only under the usual resonance conditions but at fields far from resonance also.

In the model we distinguish, somewhat arbitrarily, between ballistic and diffusing electrons depending on whether they have or have not lost their momentum memory since the excitation at the surface. The excited magnetization of the diffusing electrons gives rise to the electron-spin resonance. At high temperatures where the momentum mean free path is short this is the only significant mode. At resonance the wave vector is purely real, while off resonance it has equal real and imaginary parts. This was demonstrated by the temperature dependence of the enhanced transmission at resonance (TESR) and off resonance (TFMR). At low temperature the diffusion is modified by the presence of a strong magnetic field resulting in an anisotropy of the penetration depth of the ESR. This is reflected in a strong decrease of the transmitted ESR of foils thicker than the reduced penetration depth, $\delta_{\text{eff}}/\omega_c\tau$ in the parallel static field geometry. While the anisotropy of the TESR amplitude is thus explained, the reason for the observed change in the phase of the residual resonance is not clear and involves Fermi-liquid effects on the spin diffusion coefficient.

The ballistic electrons give rise to propagating modes, Larmor waves, attenuated by the momentum mean free path. These modes originate in the coherency of the Larmor precession of electrons with similar velocity components along the static magnetic field. In the frequency range $|\omega-\omega_0|\tau>1$ the Larmor waves represent the major component of the nonequilibrium magnetization. The enhanced spin transmission spectrum is dominated by oscillations reflecting the variation of the Larmor wavelength with magnetic field. The analysis of the Larmor wave spectrum of copper with the static field oriented around the [100] direction shows that in this case the wavelength is determined by tip electrons with velocities parallel to the static field. In other geometries the situation is more complicated and no analysis was attempted. Finally we have suggested that due to the particular geometry of the excitation via a ferromagnetic layer longitudinal waves may also be excited, a nonoscillating part of the transmission spectrum is attributed to such waves.

Larmor waves have been observed in copper, gold, and tungsten showing that it is a general phenomenon occurring at low temperatures in pure metals. In the present model and in the analysis of the experiments many rough approximations were assumed and we feel that an extension of this work may be a promising field of research.

## ACKNOWLEDGMENTS

The experiments reported in this work were carried out at the Laboratoire de Physique des Solides at Orsay, France, with the support of the Centre National de la Recherche Scientifique. Part of this work was performed in collaboration with Dr. P. Monod to whom I am greatly indebted. I am very grateful to Dr. M. Belessa from Laboratoire de Physique des Solides, Orsay, France, for preparing the gold single crystal and to Dr. B. Maxfield from Cornell University, Ithaca Laboratory of Atomic and Solid State Physics and Materials Science Center, for supplying the high-purity tungsten single crystal.

---

*Laboratoire associé au CNRS.

[1]F. J. Dyson, Phys. Rev. 98, 349 (1955).
[2]S. Schultz and G. Dunifer, Phys. Rev. Lett. 18, 283 (1967).
[3]P. M. Platzman and P. A. Wolff, Phys. Rev. Lett. 18, 280 (1967).
[4]A. Wilson and D. R. Fredkin, Phys. Rev. B 2, 4656 (1970).
[5]G. L. Dunifer, D. Pinkel, and S. Schultz, Phys. Rev. B 10, 3159 (1974).
[6]D. L. Dunifer, M. R. Patisson, and T. M. Hsu, Phys. Rev. B 15, 315 (1977).
[7]M. B. Walker, Can. J. Phys. 53, 165 (1975).
[8]M. Ya. Azbel', V. I. Gerasimenko, and I. M. Lifshitz, Zh. Eksp. Teor. Phys. 31, 357 (1956) [Sov. Phys. JETP 4, 276 (1957)].
[9]M. Ya. Azbel', V. I. Gerasimenko, and I. M. Lifshitz, Zh. Eksp. Teor. Phys. 35, 691 (1958) [Sov. Phys. JETP 8, 480 (1959)].
[10]A. Jánossy and P. Monod, Phys. Rev. Lett. 37, 612 (1976).
[11]G. B. Teitelbaum, Sov. Phys. JETP 36, 176 (1973).
[12]E. A. Kaner and V. F. Ganthmaker, Usp. Fiz. Nauk 94, 193 (1968) [Sov. Phys. JETP 11, 81 (1968)].
[13]V. F. Ganthmaker and E. A. Kaner, Zh. Eksp. Teor. Phys. 48, 1572 (1965) [Sov. Phys. JETP 21, 1053 (1965)].
[14]T. G. Phillips, G. A. Baraff, and P. H. Schmidt, Phys. Rev. B 5, 1283 (1967).
[15]A. Jánossy and P. Monod, Solid State Commun. 18, 203 (1976).
[16]R. H. Silsbee, A. Jánossy, and P. Monod, Phys. Rev. B 19, 4382 (1979).
[17]D. S. Montgomery and M. B. Walker, Phys. Rev. B 19, 1566 (1979).
[18]D. Pinkel and S. Schultz, J. Magn. Res. 22, 509 (1976).
[19]M. Lampe and P. M. Platzman, Phys. Rev. 150, 340 (1966).
[20]R. B. Lewis and T. R. Carver, Phys. Rev. 155, 309 (1967).
[21]Y. Yafet, Solid State Phys. 14, 1 (1963).
[22]R. B. Lewis and T. R. Carver, Phys. Rev. Lett. 12, 693 (1964); N. S. VanderVen and R. T. Schumaker, *ibid.*, 12, 695 (1964).
[23]Cu: ASARCO 99.999%; Au: COMINCO 99.999%, Montreal Québec, Canada; Cu, Ag, Au polycrystalline foils, Material Research Co. "Marz" grade, Orangeburg, N.Y. 10962, USA.

[24] *Amorphous Magnetism*, edited by H. O. Hooper and A. M. deGraaf (Plenum, New York, 1973).
[25] S. Schultz and C. Latham, Phys. Rev. Lett. 15, 148 (1965).
[26] D. Lubzens, M. R. Shanabarger, and S. Schultz, Phys. Rev. Lett. 29, 1387 (1972).
[27] P. Monod and A. Jánossy, J. Low Temp. Phys. 26, 311 (1977).
[28] L. D. Flessner, D. R. Fredkin, and S. Schultz, Solid State Commun. 18, 207 (1976).
[29] P. M. Platzman and P. A. Wolff, *Waves and Interactions in Solid State Plasmas in Solid State Physics,* (Academic, New York, 1973), Vol. 13, Suppl.
[30] A. Jánossy (unpublished).
[31] G. A. Baraff and T. G. Phillips, Phys. Rev. Lett. 24, 1428 (1970).
[32] M. R. Halse, Philos. Trans. R. Soc. London Sect. A 265, 507 (1969).
[33] A. Jánossy and J. Kollár, J. Phys. F 8, 2429 (1978).